BEAM DYNAMICS STUDIES FOR THE FRIB DRIVER LINAC*

Q.Zhao#, M.Doleans, F. Marti, T.P. Wangler, X.Wu, R.C.York, NSCL, East Lansing, MI 48824, USA
J. Qiang, LBNL, Berkeley, CA 94720, USA

Abstract

A driver linac has been designed for the proposed Facility for Rare Isotope Beam (FRIB) at the Michigan State University. The superconducting driver linac will accelerate stable isotope beams to energies ≥200 MeV/u with a beam power up to 400 kW for the production of rare isotope beams. This driver linac consists of a front end and two segments of superconducting linac connected by a charge stripping section. End-to-end beam simulation studies with high statistics have been performed using the RIAPMTQ and IMPACT codes on high performance parallel computers. These studies include misalignment of beam elements, rf amplitude and phase errors for cavities, and stripper thickness variation. Three-dimensional fields of the superconducting solenoids and cavities were used in the lattice evaluation. The simulation results demonstrate good driver linac performance. No uncontrolled beam losses were observed even for the challenging case of multiple charge state uranium beam acceleration. The beam dynamics issues will be discussed and the detailed beam simulation results presented.

INTRODUCTION

Facility for Rare Isotope Beam (FRIB) [1] will be a U.S. Department of Energy's national user facility located on the Michigan State University (MSU) campus. The proposed FRIB facility is based on a heavy-ion linac with a minimum energy of 200 MeV/u for all ions at a beam power of 400 kW. This advanced facility will have a production area, a three-stage fragment separator, three ion-stopping stations, and a reaccelerator to provide world-leading scientific opportunities with rare isotope beams. Figure 1 shows a schematic layout of the facility. Upgrade options are also built into the base facility design. More information on the facility can be found in [1] and [2].

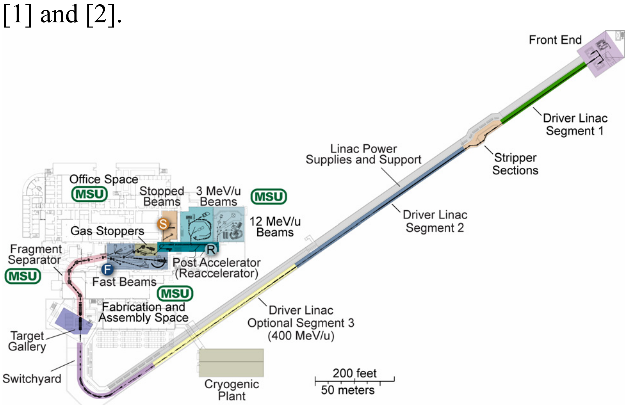

Figure 1: Schematic layout of the FRIB national user facility accelerator complex proposed at MSU.

* Supported by Michigan State University and Dept. of Energy under contract numbers DE-FG02-07ER41479 and DE-FG02-08ER41554
#zhao@nscl.msu.edu

DRIVER LINAC LATTICE

The cw heavy-ion driver linac [1,2] consists of a room temperature front end and two segments of superconducting (SC) linac connected by a charge stripping and selection section. Additional space was reserved for a possible future upgrade to 400 MeV/u.

Design considerations The proposed linac design is based on the goal of constructing a reliable, low-maintenance, state-of-the-art accelerator with proven technology and robust operating stability that will minimize downtime and ensure production of intense beams for world-class experiments. The design of the driver linac is largely determined by the requirement of a 200 MeV/u, 400 kW uranium beam, and the need to accelerate a wide range of ions while limiting the uncontrolled beam loss below 1 W/m for the cw, high power SC machine to facilitate hands-on maintenance. The accelerator lattice design must provide adequate transverse and longitudinal acceptance. To achieve the required primary beam power on the production target for the heaviest ions, beam with two charge states will be selected and accelerated in the front end and segment 1. Up to five charge states will be accelerated in segment 2. Uranium will present the greatest challenge, as the beam will consist of two charge states (33+ & 34+) in segment 1, and five charge states (77+ to 81+) in segment 2. Hence, the design was primarily focused on the uranium.

Computing codes Several codes were used in the driver linac lattice design and particle tracking. The front end simulations were performed using RIAPMTQ (a parallel version of PARMTEQ with additional features) and TRACE3D. The SC linac lattice was designed based on an in-house developed code. DIMAD was used for linac and beam line misalignment and correction, and for high-order beam optic design together with COSY. End-to-end beam simulation studies with high statistics have been performed using the RIAPMTQ and IMPACT codes [3] on high performance parallel computers.

Front end The dc ion beam from a high performance electron cyclotron resonance ion source will be analyzed by an achromatic charge-to-mass selection system. The selected ion beam will then be bunched by a multi-harmonic buncher in the low energy beam transport line and matched into the Radio Frequency Quadrupole (RFQ). The 80.5 MHz RFQ will accelerate the beam from 12 keV/u to 300 keV/u providing beam velocities appropriate for injection into the SC linac. A medium energy beam transport system will then match the beam into the SC linac.

SC linac Beam from the front end will be injected into the SC linac. Four types of accelerating structures in forty-five cryomodules were used to achieve a final energy of >200MeV/u in the segment 1 and segment 2. Figure 2 illustrates the schematic layout of the cryomodules for each type. Segment 1 has fourteen cryomodules. The first two cryomodules, each containing eight 80.5 MHz β_{opt}=0.041 λ/4 cavities and seven 10-cm long solenoids boost the beam to ~1.3 MeV/u. The remaining 12 cryomodules, each containing eight 80.5 MHz β_{opt}=0.085 λ/4 cavities and three 50-cm long solenoids further accelerate the beam to 17.5 MeV/u before stripping. Two types of cryomodules are used for segment 2. One cryomodule type has six 322 MHz β_{opt}=0.285 λ/2 cavities and one 50-cm long solenoid and the other type has eight 322 MHz β_{opt}=0.53 λ/2 cavities and one 50-cm long solenoid. With twelve of first type and nineteen of second type of cryomodule, segment 2 delivers a final beam energy of at least 200 MeV/u with a beam power of 400 kW. The uranium beam energy gain along the SC linac is also shown in Figure 2.

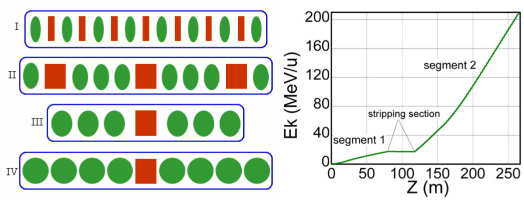

Figure 2: (left) Schematic layout of the four types of cryomodules (Green ellipses for cavities and brown rectangles for solenoids; I II for segment 1 and III IV for segment 2). (right) Uranium beam energy gain along the SC linac.

Longitudinal acceptance Beams with multiple charge state acceleration exhibit a larger effective longitudinal emittance due to the different longitudinal motion of each charge. Therefore, a larger longitudinal acceptance for each segment is required in the lattice to avoid beam loss. The calculated longitudinal acceptance, as shown in Figure 3, is about 30 and 140 π-ns-keV/u for segment 1 and segment 2, respectively. The ratio of the longitudinal acceptance to beam emittance that includes 99.99% of total about 1.6 million multi-charge-state particles at the entrance of segment 1 is about five, and that of segment 2 is about fifteen.

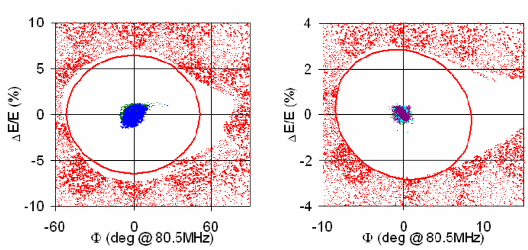

Figure 3: Longitudinal acceptance of segment 1 (left) and segment 2 (right) together with the sampled input beam.

Three dimensional fields Three dimensional fields for the SC solenoids and accelerating cavities were employed in the beam simulations to better evaluate the lattice performance. The solenoid fields were obtained from POISSON and checked with measured data from a similar configuration. Compared to the hard-edge model, the 3D solenoid fields require a few percent higher fields to achieve same focusing effect. Both MAFIA and ANALYST were used to obtain the 3D fields for each of the four types of SC cavities. As expected, the beam received a vertical kick (along the cavity conductor direction) when passing the 3D fields for both the λ/4 cavities due to the azimuthal asymmetric nature of the fields from λ/4 cavities. These kicks were compensated properly using the dipole windings located in the solenoids. Without correction for the kicks, the amplitude of the centroid orbit oscillation will continue to increase along the linac and eventually degrade the beam quality.

END-TO-END BEAM SIMULATIONS

End-to-end beam dynamics simulations have been performed starting from the entrance of LEBT, through subsequently RFQ, MEBT, segment 1, charge stripping and selection, segment 2, beam delivery line, up to the production target. For high statistical runs, a total of two million macro-particles were generated from a 4D water-bag distribution in the transverse plane and a uniform distribution in longitudinal plane. Based on the measurements of the VENUS ion source at LBNL, a dc beam with an initial normalized transverse rms emittance of 0.1 π-mm-mrad and an energy spread of 0.08% was assumed, and two-charge-state (33+ & 34+) uranium beam with total current of 12pμA was selected. About 82.5% of injected beam was accelerated by the RFQ with the rest lost in MEBT. After charge stripping, a total of five charge states (77+ to 81+) that occupy 85% of the total beam were selected and injected into segment 2. The other charge states (15% of the beam) were collimated in the selection section. Each end-to-end simulation was about two hours on high performance parallel computers with sixteen processors.

Machine error specifications The main machine errors are specified in Table 1. A uniform distribution was assumed for beam element misalignment, beam position monitor (BPM) errors, and stripper thickness variation. A Gaussian distribution truncated at ±3σ was used for rf phase and amplitude errors. A displacement of ±1 mm for cold element was chosen based on the experience at the TRIUMF and LNL. All error specifications listed in Table 1 are readily achievable.

Table 1: Error Specifications in the Beam Simulations

Name	Tolerance	Distribution
Cold element displacement	±1 mm	Uniform
Warm element displacement	±0.4 mm	Uniform
Warm element rotation	±2 mrad	Uniform
RF amplitude fluctuation	±1.5%	Gaussian (σ=0.5%)
RF phase fluctuation	±1.5°	Gaussian (σ =0.5°)
Stripper thickness variation	±10%	Uniform
BPM uncertainty	±0.4 mm	Uniform

When a misalignment is introduced, the beam centroid will be distorted leading to beam envelope growth and an emittance increase. An alignment correction procedure using room temperature BPMs between cryomodules and dipole windings in each SC solenoid was used to limit the central orbit distortion.

Results of error studies A total of 300 different seeds have been performed for the linac end-to-end multi-charge-state uranium beam simulations with errors specified in Table 1. About 1.6 million particles were tracked in each seed run. The results of these simulations are summarized in Figure 4 and Figure 5. Figure 4 shows the evolution of beam envelopes along the SC linac with and without errors, together with the minimum aperture. The blue curve, corresponding to simulations with errors included, is the maximum envelope for any of the seeds at each location. Even with the specified errors, the maximum beam envelope does not exceed ¾ of the linac aperture. The 99.99% longitudinal emittance along the linac with and without errors is shown in Figure 5. The emittance at the exit of segment 2 is three times larger than that at the entrance of segment 1 even without errors included. This growth is mainly due to the larger footprint of the multi-charge-state beam in the longitudinal phase space, since the growth is much smaller for each single charge state beam. With errors applied, the emittance growth exceeded one order of magnitude. However, no uncontrolled beam losses were observed for all seed runs. The corresponding transverse emittance growth, not shown here, is about 40% without errors and a fact of two with errors included.

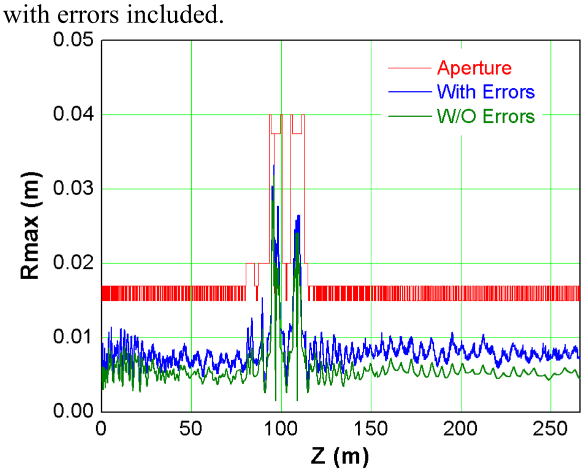

Figure 4: Beam envelopes of a multi-charge-state uranium beam with and without errors along SC linac, together with the minimum linac aperture.

To test the robustness of the design, simulations with errors twice larger than those listed in Table 1 were performed. Among 400 seeds runs, 85% of the runs did not have any beam losses, and 98% of the runs had beam loss below 1 W/m. With the specified tolerances in Table 1, rf errors generally did not impact beam in the transverse plane but mainly in the longitudinal plane, while misalignment only impacted beam in the transverse plane and no effects on the longitudinal plane. But with twice the error specifications, rf errors in segment 2 had a similar impact on transverse as misalignment largely because in this case a large longitudinal emittance developed in segment 1 was substantially increased by passing through stripper sufficient to coupled into transverse plane in segment 2. As a consequence, longitudinal emittance control is the key to minimizing beam losses.

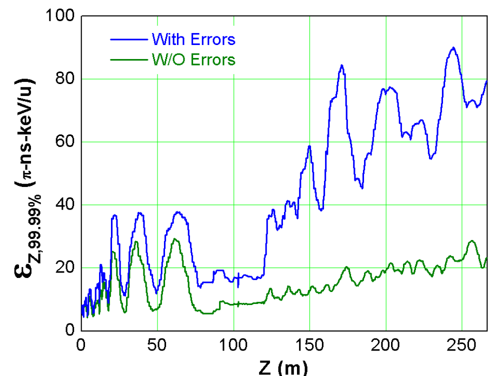

Figure 5: Longitudinal emittances (including 99.99% of all 1.6 million tracked particles) of multi-charge-state uranium beam with and without errors along the SC linac.

Outlook Future developments in beam dynamics simulation will build realistic models for each element, which involves but not limited to modelling high intensity beam formation and its transport from the ion source, improving charge stripping models, introducing realistic beam collimation models, include real operating conditions, and incorporate measured beam information as feedback. This will be very beneficial for commissioning as well as operation by helping to optimize the machine set-up for different ions.

SUMMARY

Detailed beam dynamics simulation studies that include misalignment of beam elements, rf amplitude and phase errors for cavities, and stripper thickness variation with three dimensional beam elements fields have been performed. These studies together with the engineering and cost/benefit analyses (not covered in this paper) show the proposed design is robust with minimization of beam losses, enhanced reliability, and low cost.

ACKNOWLEDGMENT

We thank K. R. Crandall, J. H. Billen and R. Ryne for providing the RIAPMTQ code and helpful discussions, and D. Gorelov for performing MAFIA 3D fields.

REFERENCES

[1] R.C. York, "FRIB: A New Accelerator Facility for the Production of and Experiments with Rare Isotope Beams", these proceedings.
[2] X. Wu, et al., "The Superconducting Driver Linac for the Proposed MSU FRIB Project", these proceedings.
[3] T.P. Wangler et al., "The RIAPMTQ/IMPACT Beam-Dynamics Simulation Package", PAC'07, p.3606.